MEMS Wireless Transceiver for Use of Non-Invasive System Diagnostics

Toluwaleke Olutayo, Jessica Ondrizek, and Justin Phelps

Dept. of Electrical and Computer Engineering
University of Central Florida, Orlando, Florida, 32816-2450

Abstract **— The purpose of this project is to design and test a transceiver that operates in the 27 MHz ISM band to communicate with a MEMS sensor. The solution is expected to be used as a method of performing non-invasive testing on motor systems. This paper discusses the challenges faced and design procedure used through the course of the two-semester project.**

Index Terms **— Fast Fourier transforms, microelectromechanical systems, microelectromechanical devices, radio transceivers.**

I. Introduction

As the size of electrical components becomes smaller and smaller, the future of electronics lies not in nanotechnology, but in microtechnology. The marketability of MEMS, or microelectromechanical systems, is increasing as the field expands and new applications are developed. Most of the MEMS products developed are sensors which relate changes in capacitance, resistance, or voltage to changes in the environment. Despite the complexity of these devices, they are worthless without a method of reliably communicating with the sensor.

In this project, a transceiver will be designed to communicate with a sponsor-provided MEMS sensor that will be positioned on a motor a specified distance away. In this setup, the transceiver will wirelessly communicate with the sensor via a 27 MHZ frequency in order to monitor the health of the motor in a non-invasive manner.

Non-invasive testing is typically accomplished by means of small sensors that are positioned within the structure or system and remain there throughout the life of the unit in question. These sensors typically monitor the frequency and amplitude of a system's vibration and pass these values to a computer for analysis of the data. Unusual or extreme shifts in these parameters can indicate that a system may be malfunctioning or needs maintenance.

Non-invasive sensor devices have already been designed and are currently available on the market. However, the available designs operate at frequencies far beyond the ISM band. One of the biggest issues with devices operating at this frequency is interference. To counteract the effects of interference, the transmitter and receiver operate at slightly different frequencies and must perform modulation to communicate. Because pre-existing designs already functions at high frequencies, it is undesirable to modulate these signals to even higher frequencies.

To avoid issues caused by operation at higher frequencies, this project aims to communicate with a sponsor-provided MEMS sensor via radio frequencies. This goal is to be accomplished by sending high-power radio signals to the MEMS sensor for excitation before switching to a receiving mode to gather data from the sensor. The response of the MEMS sensor is frequency variant, and this variance in frequency will allow us to determine the overall health of the system. This will be accomplished by taking the received frequency response of the system and applying a fast Fourier transform (FFT) to the signal and looking for frequencies that are outside of the standard value. Once the FFT has been performed on the systems microcontroller, the microcontroller will relay the data to a computer where a graph will be plotted to display the characteristics of the systems status.

The completed design package will contain a fully integrated system. The system will consist of a printed circuit board (PCB) with embedded microcontroller that provides bidirectional communication to the sensor through the 27 MHz antenna. The PCB will also be capable of interfacing with the PC via serial USB communication. The system will have a launchable application on the Windows platform to provide the user with system diagnostics. The goal of this project is to create a fully functional and reliable piece of test equipment that will allow the sponsor to easily monitor the health of their systems.

II. STANDARDS

Without regulatory standards, many engineering designs would be incompatible with each other, be wildly varied in their designs, or be hazardous to the public or environment. The establishment of engineering standards and design constraints, typically by associates like the Institute of Electrical and Electronics Engineers (IEEE) and the American National Standards Association (ANSI), ensures that engineers have a common and sound approach to designing. The standards and constraints which have the most bearing on our projects are discussed in the sections below.

A: IEEE Standard 1149.1-2001: IEEE Standard Test Access Port and Boundary-Scan Architecture

This standard relates to the maintenance, testing and support of assembled printed circuit boards (PCB) and the testing of internal circuits [1]. A standard interface must be selected so that instructions can be communicated through it. One of the test features dictated by this standard is the boundary-scan register. The boundary scan register is a testing method which ensures that the device can respond to a set of instructions designed to test the components of the printed circuit board (PCB).

To ensure that the PCB works as expected, a series of tests were designed to check the functionality of the circuit. JTAG enabled devices, through a series of tests are specifically designed to check that the connections on the printed circuit board match that of the actual design. This step of checking the connections on the PCB through these specially designed tests help to ensure that circuit works as expected. This is an important step as it verifies the correctness of the design of the device and ensures proper functionality of the circuit. If the PCB design fails these tests, it must be redesigned and retested.

B: IEEE Standard for Safety Levels with Respect to Human Exposure to Radio Frequency Electromagnetic Fields, 3 kHz to 300 GHz

The IEEE standard for safety defines the safe levels of human exposure to radio frequency electromagnetic fields [2]. These recommendations ensure that the public is protected from the adverse effects of exposure to electromagnetic fields in the radio frequency range of 3 kHz to 300 GHz. The recommendations are divided into two classifications: basic restrictions (BR) and maximum permissible exposure values (MPE). The purpose of this standard, as described by the IEEE, is to significantly limit the effect of electromagnetic field (EMF) energy on human health.

The basic restrictions can be further subdivided into three categories: internal fields, specific absorption rate (SAR), and current density. Internal fields are defined as emission of electrons because of an electrostatic field. Specific absorption rate is defined as the rate of absorption of radio frequency electromagnetic energy by a body. According to FCC regulations, SAR is tested by using the highest power level in all the frequency bands and testing their effects on models of different human tissues. Finally, current density emission relates the thermal energy to current.

For radio frequency transmissions within the frequency range of 3 kHz to 5 MHz, the major health concern is painful electrostimulation. For frequency transmissions within the frequency range of 100 kHz to 300 GHz, the IEEE regulations focus on minimizing adverse health effects that are associated with heating. Because the device is designed to work at 27 MHz, it falls within the 100 kHz to 300 GHz range. It should be mentioned that the IEEE standard does not consider the sensation of heating as adverse. However, the heating of body tissues is an adverse side effect. As such, rules and guidelines pertaining to type of waveforms, duty factor, and transmission time must be established.

III. SYSTEM COMPONENTS

Given that this system is large and utilizes many different components, it would be impossible to describe all of the components in depth. This section will serve to discuss only the main parts of the design.

A. MICROCONTROLLER

The chosen microcontroller is the Texas Instrument TMS320F28335. The unit was chosen because of its high processing capability, integrated on-board analog-to-digital converter, and low number of peripheral components required for the function of the device. Another advantage of this device is that it offers 63 GPIO pins in order to control and monitor the system. A final advantage of this device is that a sample schematic provided for the connectivity of this device. This ensures that the device functions as required and minimizes design time.

Because the device belongs to the Texas Instruments family, it can interface with a PC via a combination of multiple softwares; namely Code Composer Studio, C2000Ware, and ControlSuite. These programs may be used to control the device.

C. BANDPASS FILTERS

Two bandpass filter configurations, a fourth order and fifth order, are used in this design to reduce the noise signal and preserve the received signal. The fifth order configuration (shown in Fig. 1) is used to filter the signal being transmitted to the power amplifier stage.

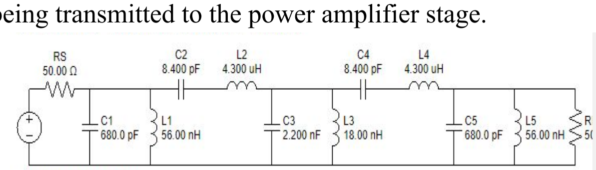

Fig. 1 Fourth order bandpass filter design

The fourth order configuration, shown in Figure 2, will be used in the filtering stage that occurs before the signal is mixed.

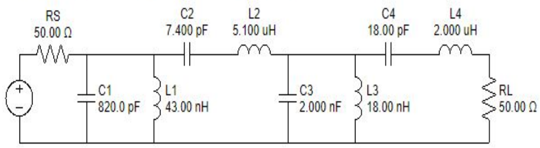

Fig. 2 Fifth order bandpass filter design

D. POWER AMPLIFIER

Since we were unable to find a suitable packaged power amplifier, one must be designed. The power amplifier will consist of multiple operational amplifiers that will be joined together to increase the current output of the device. To preserve the quality of the signal, the operational amplifiers selected are very fast relative to the output signal. The part number of the selected operational amplifier is LMH6703MAX/NOPB. This part is selected for its high frequency operation up to 1.2 GHZ and its fast slew rate of 4.2kV/us [3]. The design of the power amplifier is shown in Figure 3.

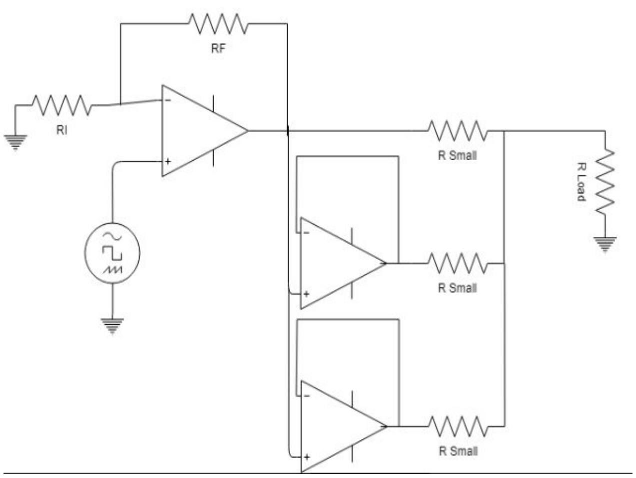

Fig. 3 Power amplifier design

The above amplifier design was selected because no high-power RF amplifiers existed in the 27 MHZ range that we needed. The solution that we came to was to use consecutive operational amplifiers by this design we can increase the current output going to the antenna.

E. DOWNCONVERTER MIXER

Because the signal being processed requires modulation, a radio frequency mixer must be used to perform the modulation. Mixers, which typically have three ports (an RF input port, a local oscillator LO input port, and intermediate frequency IF output port), operate by adding or subtracting frequency values in order to obtain a desired output frequency. In this design, a downconverting mixer is used to subtract the RF and LO inputs to obtain the desired frequency.

The downconverter mixer that was ultimately decided on is the LT5560. The LT5560 is a low power active mixer produced by Linear Technology that can support frequencies between 0.01MHz to 4GHz [4]. This component was chosen because it features a sample test circuit which can be externally matched for the desired frequency by selecting and solving for resistor, inductor, and capacitor values. Additional advantages of this part are its small footprint (it comes in a 3mm x 3mm package) and it operates within our desired temperature range.

F. LIMITER

In signal processing, limiters are circuits which attenuate (or limit) the strength of signals above a certain threshold while allowing signals below this threshold to pass unaffected [5]. In most cases, limiting is done as a safety measure. If a signal is too powerful, it can damage the equipment that it is passing into. However, limiting may also be performed to protect the integrity of the signal that is being processed and to ensure that the next stage is provided with a constant level of signal. If a signal is not limited, it could introduce undesired distortion.

The circuit will employ a series of limiters, similar to the ones shown in Fig. 4, to help process and normalize the signal to the desired amplitude and shape. By implementing limiters in the design, the decaying signal can be amplified and limited to the point where the entire signal resembles something like a square wave. After transforming the amplified signal to a square wave, it is then converted to a sine wave by filtering the signal prior to the down-conversion.

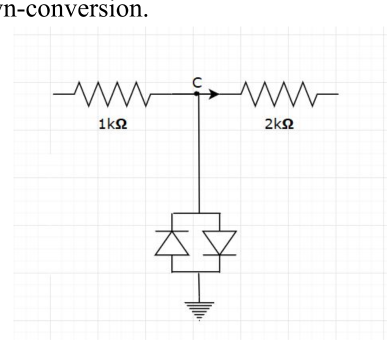

Fig. 4 Limiter design

IV. SYSTEM CONCEPT

Because the system is large and utilizes many connected components, a flowchart (shown in Fig. 5) is useful for understanding the complete design.

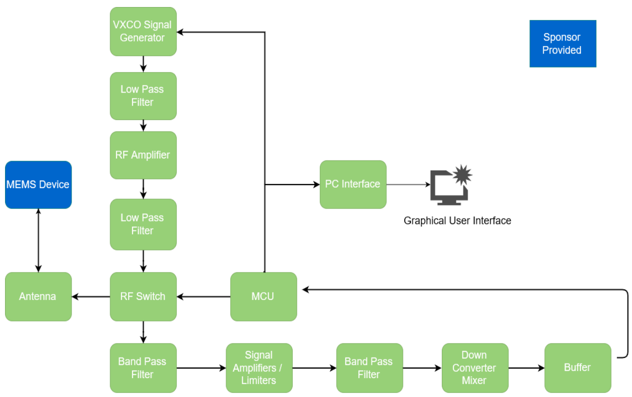

Fig. 5 Block diagram of the overall system design

The design can be divided into two distinct functions: transmitting and receiving. Some components will be used only along the transmit signal path while others may be used only during the receiving signal path. The transmitting portion of the design is visualized in the block diagram shown in Fig. 6.

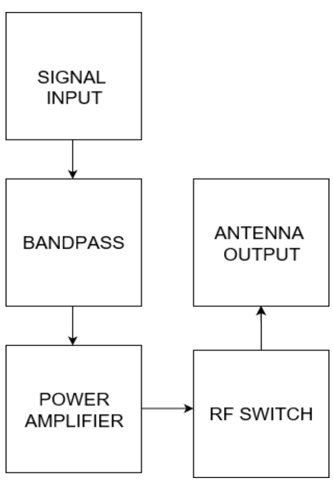

Fig. 6 Transmission Block Diagram

The signal path of the transmitting stage will originate at the microcontroller. An input or signal will be generated and then passed through a fifth order bandpass filter. The filter will ensure that the signal lies within a 25 MHz to 28 MHz range. After filtering, the signal continues to the power amplifier stage. Here, the signal passes through the LMH6703MAX/NOPB to be amplified to a sufficient level to be transmitted. After amplification, the signal is passed to the RF switch which has been configured to the 'transmit' position by the microcontroller. The signal is passed from the RF switch to the antenna for transmission to the MEMS sensor.

Similarly, the reception portion of the design is visualized in the block diagram shown in Fig. 7.

The reception signal path will originate at the antenna and the RF switch must be configured to the 'receive' position in order to pass the incoming signal to the rest of the path. After being received, the signal must be filtered. The signal passes through a fourth order Butterworth bandpass filter to cutoff any frequencies that lie outside out of the 25 MHz to 28 MHz band. After this initial filtering, the signal is passed through a buffer and limiter. These two components will help protect the rest of the circuit from dangerously high voltages transmitted by the antenna. Next, the signal enters another filtering stage. This main filtering stage serves to amplify the signal by passing it through a series of amplifiers and then clip the signal by passing it through a limiter. Through this process, the signal is transformed into the desired amplitude and frequency. The signal is again passed through a fourth order Butterworth bandpass filter to ensure that it is sufficiently clean before being mixed. After mixing the signal to the desired intermediate frequency, the signal is passed through a buffer that separates the mixer from the microcontroller. Because the microcontroller has on-board ADC capabilities, the signal is converter here before being transmitted to the PC for further processing.

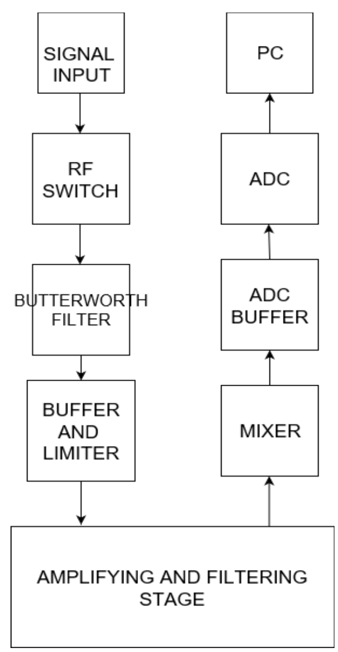

Fig. 7 Reception Block Diagram

V. HARDWARE DESIGN

A. POWER

Power is supplied to the board as +5VDC and -5VDC. Because most of the components use voltage values smaller than +5VDC, a DC/DC converter is used to step the voltage down. The TPS62400DRCR from Texas Instruments is a two-output DC/DC converter. +5VDC is supplied to the device and it is designed to output +3.3VDC and +1.9VDC. An AP2204K-3.3TRG1 voltage regulator from Diodes Incorporated is used to convert +5VDC to +3.3 analog voltage. The power supply design is shown in Fig. 8.

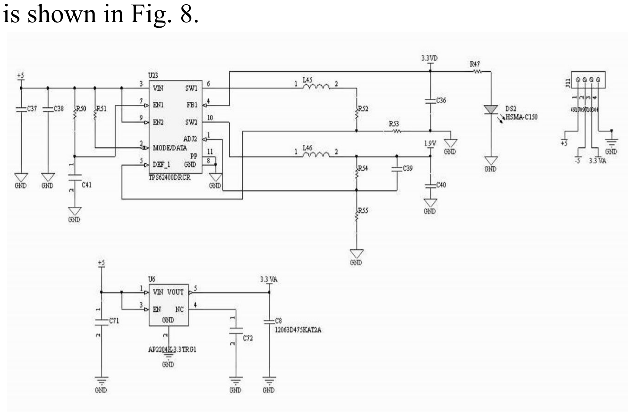

Fig. 8 Voltage conversion from +5VDC to +3.3VDC, +3.3VA, and +1.9VDC

B. OPERATIONAL AMPLIFIERS

This design uses a variety of operational amplifier designs throughout both the transmit and receive portions of the design. The three main configurations used are the unity gain amplifier, non-inverting amplifier, and inverting amplifier.

The unity gain amplifier is the simplest of these configurations. Because no resistors are placed at the operational amplifier, it produces no gain. The idealized unity gain amplifier can be described by the equation:

$$\frac{V\,out}{V\,in} = 1 \qquad (1)$$

The inverting amplifiers are used most in the design at the amplification stage where they are cascaded into one another to cancel out the effect of inversion and to increase the overall gain. The idealized gain equation, which is given as:

$$Av = \frac{Rf}{Rin} \qquad (2)$$

This equation can be used to find the amount of gain occuring at each amplifier. Rf was chosen to be 942 kΩ and Rin was chosen to be 20 kΩ to obtain a gain of approximately 47 at each amplifier. These operational amplifier designs are shown in Figure 9.

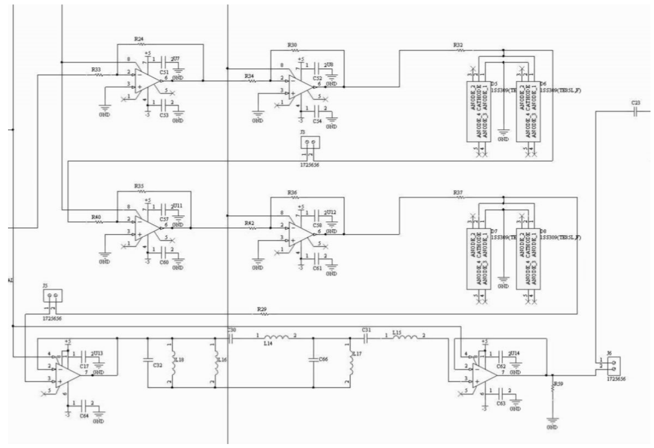

Fig. 9 Inverting amplifiers with a gain of 47

The non-inverting amplifier is used throughout the design and the desired gain varies. The idealized gain equation is given as:

$$Av = 1 + \frac{Rf}{Rin} \qquad (3)$$

Because the operational amplifiers used throughout the design serve a variety of purposes, multiple operational amplifiers were used, including the LMH6703MAX/NOPB from Texas Instruments, LT6202CS5#TRMPBF from Analog Devices, and LT1206CS8#PBF from Analog Devices. All amplifiers were chosen because they are capable of operating at sufficiently high frequencies and require a +/-5VDC supplies. The LMH6703MAX/NOPB and LT1206CS8#PBF require additional voltage inputs in order for the devices to be enabled or disabled.

C. RF SWITCH

The RF switch is the key to transitioning between the transmit and receive capabilities. As such, it is critical that the switch used can operate as required. The RF switch that was chosen for the design is the HMC199AMS8E from Analog Devices. It was chosen because it is a single pole double throw (SPDT) switch that allows for a single input to switch between two outputs. Utilizing a single enable bus helps simplify the software to control the switching.

D. DOWNCONVERTER MIXER

As previously discussed, the LT5560 downconverting mixer from Linear Technologies was chosen for this design. This was largely due to the device being capable of supporting frequencies in the MHz range and the datasheet having a test circuit that could be modified to accommodate different frequencies. The mixer design, as shown in Figure 10, is largely based off of the layout given in various test circuits from the LT5560 datasheet [6]. However, the components values have been calculated to mix at the required frequency. The equations required to calculate new values for lumped element matching are as follows:

$$Lo = \frac{\sqrt{RA * RB}}{2 * \pi * fc} \quad (4)$$

$$Co = \frac{1}{2 * \pi * fc * \sqrt{RA * RB}} \quad (5)$$

where RA and RB are the terminating resistances and fc is the desired center frequency.

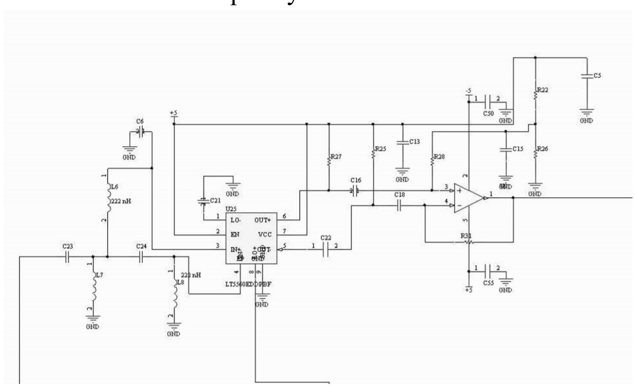

Fig. 10 Downconverting mixer design

VI. SOFTWARE DESIGN

The software design concept revolves around protecting signal integrity and providing data accuracy and precision by adding redundancy to the system. The software will achieve this purpose through three main approaches:

(1) Perform an analog to digital conversion of the received signal,
(2) Provide precise switching frequency for the square wave, and
(3) Enable other peripherals on the circuit board when required.

To perform the analog to digital conversion, the ADC component of the MCU samples the signal received from the ADC buffer at a minimum of two times the transmitting frequency rate in order to satisfy the Nyquist sampling criterion. The signal from the receiver is passed through a train of filters and limiters and this helps ensure that there are no aliasing effects during the ADC process that can compromise signal integrity. Then, the microcontroller passes the information to the computer via the UART (SCI) communication protocol for further processing. A JavaScript program on node.js performs a fast Fourier transform on the received ADC values, and then the resonant frequency is obtained by scanning the array for the frequency component with the highest magnitude. The resonant frequency is then transmitted back to the MCU which then updates the switching frequency of the square wave. This process is repeated a few times in order to obtain sufficient data points to accurately perform a spectral analysis of the received signal.

A simple graphical user interface was also designed in Javascript. The purpose of this GUI was to interface with the serial communication port to graph the values of the received signal in real time. In an attempt to avoid unnecessarily switching back and forth between screen view, the signal is simultaneously displays the signal in both the time domain and the frequency domain. The GUI automatically tracks the most recent inputs, but it also offers the option to pause the incoming signals and scroll back through previous values for analysis.

The general functionality of the software design is broken up into three stages as discussed in the introductory paragraph of this section. Shown in the image below is the MCU implementation of switching and updating the frequency of the square wave that is then subsequently filtered. The MCU waits to get the resonant frequency from the computer. Then, it updates the switching frequency and consequently the frequency of the squarewave. The period of the squarewave is configured such that it is on half of the time and off for the other half. This results in a 50% duty cycle squarewave being generated.

```
        while(SciaRegs.SCIFFRX.bit.RXFFST !=1)
        {

        }

        ReceivedChar = SciaRegs.SCIRXBUF.all;
        Resonant_Freq = ReceivedChar;

       if (Resonant_Freq % 0!=0)
       {
           Resonant_Freq = Resonant_Freq + 1;
       }

        scia_msg(msg);
        scia_msg_int(ReceivedChar);
        scia_msg("\r\n");

h = 1/(Resonant_Freq);
    SW_TX_MODE;
    DELAY_US(h/2);
    SW_RX_MODE;
    DELAY_US(h/2);
```

Fig. 11 Example code that controls the switching and frequency of the input square wave

The 16-bit ADC module is configured to sample at the max sampling frequency rate of 12.5MHz, well above the nyquist sampling rate of approximately 2 MHz. The FFT algorithm is implemented on 64 data points at a time and then subsequently updated as new sets of data points are sent from the MCU. This way the resonant frequency, after each implementation of the FFT algorithm, is obtained, transmitted to the computer and used to obtain the next batch of data points.

VII. PRINTED CIRCUIT BOARD DESIGN

The printed circuit board component of the project consisted of a large multilayer board that measured 6.9" across and 8.5" long. Overall, the design incorporated 273 components, most of which were SMD. Due to the number of components, voltage sources, and nets, a four-layer board was chosen for the design. The top layer consisted solely of signal traces and SMD components which were soldered to the PCB and the second layer was reserved for the +5V, -5V, +3.3VD, +3.3VA, and +1.9V planes. The third plane was reserved for the ground plane and the bottom plane was reserved exclusively for traces.

Due to the frequency constraints of the project, sources of stray capacitance and inductance were a main concern. The copper used in the PCB had the potential to introduce introduce intrinsic inductance and capacitance that could exceed the values required in the design. As such, the length, width, height, and thickness of the copper trace needs to be considered. The inductance value of a length of copper wire can be approximated by:

$$L(nh) = 2ln(\frac{5.98h}{0.8w} + t) \qquad (6) \qquad [7]$$

and the capacitance can be approximated by:

$$C(pf) = \frac{0.264(r + 1.41)}{ln(\frac{5.98h}{0.8w} + t)} \qquad (7)$$

Additional considerations include the characteristic impedance, which describes the capacitive and inductive behavior of the transmission line as the voltage and current waves propagate along the length, and the dielectric of the PCB material [8]. The dielectric of the PCB material is easier to account for, as most PCBs are made of FR-4 which has a typical permeability of 4.5.

Just as copper traces can introduce capacitance and inductance effects, vias can introduce similar effects [7]. The inductance of the vias can be approximated by:

$$L(nH) = \frac{h}{5}[1 + ln\frac{h}{5}] \qquad (8)$$

and the capacitance of the vias can be approximated by:

$$C(pF) = \frac{0.055rhd1}{(d2 - d1)} \qquad (9)$$

where *h* is the height of the via, *d* is the diameter of the hole, *d1* is the diameter of the top layer of the trace, and *d2* is the diameter of the trace of the bottom layer.

As a result, steps were taken to minimize the amount of noise experienced between components and to minimize the degradation of the signal. Design decisions included:

(1) Minimizing the length and amount of looping of the traces connecting two components,
(2) Placing bypass capacitors as close as possible to the voltage supplies, and
(3) Using traces to connect components when they were placed close enough to allow for it, but using vias to connect to various planes as required.

Because the design was so large, there was a high likelihood that sections of the PCB would not function as required. In an attempt to ease the testing of the board, female header pins were placed strategically throughout the board. Connectors were placed at the output of the power amplifier, input to the RF switch, between the Butterworth filter and amplifying stage, between stages of amplification, at the input of the downconverter mixer, at the ADC buffer, at boot resistors, and at the USB interface. The use of these pins ensure that key stages of the design could be probed and measured independently of one another if required.

Another testing technique which was used was the design of two daughter cards - one for transmission and one for reception - which would plug into a TMS320F28335 Experimenter Kit from Texas Instruments. The design of these two boards was nearly identical to the layout of the four layer PCB, but with some modifications to make the design simpler:

(1) The daughter cards were limited to two layers - the top layer for SMD components and signal traces and the bottom layer was used exclusively for signal traces.
(2) Female header pins were used to supply power and grounding to the board via signal traces.
(3) Female header pins were strategically measured and placed along the edge of the board so that they could directly interface with the test pins on the experimenter's kit.

VIII. CONCLUSION

The design of this project posed several large design challenges that we have been able to overcome. Issues such as high frequency effects on passive components as well as limitations of RF amplifiers (such as gain bandwidth constraints for amplifying) have been carefully researched and designed around. Another main difficulty faced were limitations in the component selection. The 27 MHz frequency of operation is below the RF range that components and filters are typically designed for, but above the operation range that individual components can operate in. The frequency constraints imposed by components lead to extra design work that typically would not be necessary had the frequency been shifted either higher or lower range.

Acknowledgement

The authors first wish to acknowledge the assistance and support provided by Dr. Reza Abdolvand and his graduate team. His guidance and his generosity with his time and advice were invaluable.

We would also like to acknowledge and thank Jacob Clevenger and Dallas Marcone for their input and guidance in the design of the software and PCB.

Finally, the authors wish to offer our thanks and gratitude to the professors and coworkers who have set aside time in their busy schedules to review our project.

BIOGRAPHY

Toluwaleke Olutayo will receive his Bachelor's of Science in Electrical Engineering in August of 2019. He will pursue his Master's degree in Electrical Engineering at Boston University. He plans to focus his studies in Telecommunication.

Jessica Ondrizek will receive her Bachelor's of Science in Electrical Engineering in August of 2019. After graduation, she will transition from College Work Experience Program (CWEP) participant to full time employee in Lockheed Martin's test engineering department. She hopes to eventually work in space programs and obtain her Master's degree in Electrical Engineering.

Justin Phelps will receive his Bachelor's of Science in Electrical Engineering in August of 2019. Following graduation, he plans to attend the University of Central Florida to obtain his Master's degree and continue his research under Dr. Reza Abdolvand. He plans on pursuing his doctorate degree and a career in teaching.

References

[1]"1149.1-2013 - IEEE Standard for Test Access Port and Boundary-Scan Architecture - IEEE Standard", *Ieeexplore.ieee.org*, 2019. [Online]. Available: https://ieeexplore.ieee.org/document/6515989. [Accessed: 21- Apr- 2019].

[2]"P1666 - Standard for Standard SystemC Language Reference Manual", *Standards.ieee.org*, 2019. [Online]. Available: https://standards.ieee.org/project/1666.html. [Accessed: 21- Apr- 2019].

[3]"What is Self Resonant Frequency? - everything RF", *Everythingrf.com*, 2019. [Online]. Available: https://www.everythingrf.com/community/what-is-self-resonant-frequency. [Accessed: 21- Apr- 2019].

[4]T. Instruments, "LMH6703MA/NOPB Texas Instruments | Integrated Circuits (ICs) | DigiKey", *Digikey.ca*, 2019. [Online]. Available: https://www.digikey.ca/product-detail/en/texas-instruments/LMH6703MA-NOPB/LMH6703MA-NOPB-ND/755059. [Accessed: 21- Apr- 2019].

[5]"Limiter", *En.wikipedia.org*, 2019. [Online]. Available: https://en.wikipedia.org/wiki/Limiter. [Accessed: 21- Apr- 2019].

[6]*Analog.com*, 2019. [Online]. Available: https://www.analog.com/media/en/technical-documentation/data-sheets/5560f.pdf. [Accessed: 21- Apr- 2019].

[7]"High Speed Analog Design and Application Seminar", 2019. [Online]. Available: http://www.ti.com/lit/ml/slyp173/slyp173.pdf. [Accessed: 21- Apr- 2019].

[8]"Characteristic Impedance | Transmission Lines | Electronics Textbook", *Allaboutcircuits.com*, 2019. [Online]. Available: https://www.allaboutcircuits.com/textbook/alternating-current/chpt-14/characteristic-impedance/. [Accessed: 21- Apr- 2019]